ORIGINAL RESEARCH ARTICLE

Physiologically Based Pharmacokinetic Modelling to Identify Physiological and Drug Parameters Driving Pharmacokinetics in Obese Individuals

Mattia Berton[1,2] · Sara Bettonte[1,2] · Felix Stader[3] · Manuel Battegay[1,2] · Catia Marzolini[1,2,4]

Abstract

Background Obese individuals are often underrepresented in clinical trials, leading to a lack of dosing guidance.

Objective This study aimed to investigate which physiological parameters and drug properties determine drug disposition changes in obese using our physiologically based pharmacokinetic (PBPK) framework, informed with obese population characteristics.

Methods Simulations were performed for ten drugs with clinical data in obese (i.e., midazolam, triazolam, caffeine, chlorzoxazone, acetaminophen, lorazepam, propranolol, amikacin, tobramycin, and glimepiride). PBPK drug models were developed and verified first against clinical data in non-obese (body mass index (BMI) $\leq$ 30 kg/m^2) and subsequently in obese (BMI $\geq$ 30 kg/m^2) without changing any drug parameters. Additionally, the PBPK model was used to study the effect of obesity on the pharmacokinetic parameters by simulating drug disposition across BMI, starting from 20 up to 60 kg/m^2.

Results Predicted pharmacokinetic parameters were within 1.25-fold (71.5%), 1.5-fold (21.5%) and twofold (7%) of clinical data. On average, clearance increased by 1.6% per BMI unit up to 64% for a BMI of 60 kg/m^2, which was explained by the increased hepatic and renal blood flows. Volume of distribution increased for all drugs up to threefold for a BMI of 60 kg/m^2; this change was driven by pK_a for ionized drugs and log$P$ for neutral and unionized drugs. C_{max} decreased similarly across all drugs while t_{max} remained unchanged.

Conclusion Both physiological changes and drug properties impact drug pharmacokinetics in obese subjects. Clearance increases due to enhanced hepatic and renal blood flows. Volume of distribution is higher for all drugs, with differences among drugs depending on their pK_a/log$P$.

1 Introduction

Obesity is a chronic and relapsing disease characterized by an abnormal or excessive fat accumulation. It is defined by the World Health Organization (WHO) by a body mass index (BMI) $\geq$ 30 kg/m^2 [1]. Since 1980, obesity has more than double and is recognized by WHO as an epidemic [1–3]. Obesity is an established risk factor for all-cause mortality likely mediated through its association with a wide range of chronic diseases including type 2 diabetes, cardiovascular disease, and certain cancers [4, 5].

The association between obesity and comorbidities implies that obese individuals require medications; however, guidance on how to adjust drug dosing is often lacking in both label and literature due to the under-representation of obese subjects in clinical studies [6]. To date, empirical methods that rely

---

Extended author information available on the last page of the article

Key Points

Drug pharmacokinetics in obese subjects (BMI $\geq$ 30 kg/m^2) were accurately predicted by our physiologically based pharmacokinetic framework informed with our previously developed obese population repository (i.e., 71.5% of predictions were within the 1.25-fold and none outside the twofold of clinical data).

The model predicted an average 1.6% increase in clearance per BMI unit, which was explained by an increase in hepatic and renal blood flows. The volume of distribution increased on average up to threefold for a BMI of 60 kg/m^2; this change was driven by drug properties (pK_a and log$P$).

Dosing in obese subjects needs to take into account both physiological parameters and drug properties.

on body size descriptors (e.g., total body weight, lean body weight, ideal body weight, and body surface area) together with or without a scaling factor (e.g., 1 in case of linear relationship, 0.75 in case of an allometric relationship or different one that is extrapolated from pharmacokinetic data) are used to scale the dose from non-obese to obese [7]. However, none of them can be effectively used across different medication classes simply because these methods do not account for the multiple factors that may impact drug pharmacokinetics. These factors include the physiological changes related to increasing BMI (i.e., increase in hepatic blood flow, adipose tissue, glomerular filtration rate, and modification of enzyme abundance), which impact both drug elimination and distribution. The latter is also influenced by the physicochemical properties of the drug such as log$P$ or partition coefficient. The log$P$ represents the lipophilicity of the compound in the unionized form, the pK_a or acid dissociation constant determines the ionisation state of the drug, and the log$D$ or distribution coefficient is a parameter combining log$P$ and pK_a and expressing the lipophilicity of a compound at a given pH.

Physiologically based pharmacokinetic (PBPK) modelling allows simulation of virtual clinical trials by using prior knowledge on human physiology and drug properties, thereby enabling exploration of drug disposition in virtual subjects with different degrees of obesity. The first aim of this study was to verify the capability of our PBPK framework informed by our previously developed obese population repository to predict drug pharmacokinetics in obese individuals [8]. The second aim was to determine the physiological and drug physicochemical properties driving drug disposition changes in obese individuals.

2 Methods

2.1 Physiologically Based Pharmacokinetic Model

We used our in-house whole body PBPK framework developed in Matlab® 2020a [9] to simulate the pharmacokinetics in obese subjects. Briefly, its structure consists of 18 compartments, each one representing an organ or a tissue connected to each other by blood flow rates. Drug distribution in the compartments is assumed to be perfusion limited. The prediction of tissue:plasma distribution partition coefficients is based on the method of Rodgers and Rowland [10, 11]. The generation of the virtual population relies on parameter repositories [9]. The model already contained a healthy and elderly population [12]; however for this work the PBPK framework was implemented with our developed repository summarizing the anatomical, physiological, and biological parameters for individuals with a BMI ranging from 18.5 to 60 kg/m^2 together with the corresponding parameter variability [13].

2.2 Parameters of Simulated Drugs

We carried out a thorough literature search to identify drugs with available pharmacokinetic data in obese subjects in order to verify the PBPK drug models predictions against clinically observed data. We selected ten drugs characterized by different elimination pathways including midazolam, triazolam, caffeine, chlorzoxazone, acetaminophen, lorazepam, propranolol, amikacin, tobramycin, and glimepiride. Input drug parameters were obtained from verified published PBPK models [14–21]. However, for chlorzoxazone a PBPK model was not available, therefore it was developed from scratch combining in vitro data and clinical clearance data. The parameters of the ten simulated drugs are found in the Online Supplementary Material (OSM) Table S-1.

2.3 Model Development Workflow

We followed a specific workflow to develop the PBPK drug models. First, we compiled data on anthropometric parameters, study design, and pharmacokinetic results from the available clinical trials. When more than one published study was available, we calculated the weighted mean and standard deviation of the reported pharmacokinetic parameters values. Data published in different formats (i.e., mean and standard error) were converted into arithmetic mean and standard deviation. We extracted available concentration-time profile plots using GetData Graph Digitizer® and, when needed, used these data to calculate missing pharmacokinetic parameters by using noncompartmental analysis (NCA). Once all the observed data were collected, we developed and verified the PBPK model by predicting the pharmacokinetics in non-obese subjects first after intravenous administration (if available in the literature) then after single and multiple oral administration (more detailed workflow for midazolam is reported in the OSM). All simulations were run using the same proportion of female, age, and BMI as reported in the clinical trials. The observed clinical data were visually compared against the predicted concentration-time profiles. Furthermore, we calculated the ratio of the predicted:observed pharmacokinetic parameters. Simulations were considered successful when the ratio was within the twofold error margin of the observed data [22]. The verified drug model was then used to predict the pharmacokinetics in virtual obese individuals without changing any drug parameter. Comparison with the observed clinical data was also carried out for the simulations in obese both visually and numerically; the latter was retained successful if the pharmacokinetic parameters were predicted within a twofold error margin.

When simulating the results of some clinical studies (i.e., midazolam and triazolam intravenous and oral, caffeine oral, and acetaminophen and lorazepam intravenous), the numerical inspection was considered more important than the visual inspection because the clinically observed data did not represent the mean concentration-time profile but rather reflected the individual concentration-time profile. As an additional verification step to prove that the model was able to predict the pharmacokinetic changes in obese subjects, we compared the non-obese:obese predicted ratio against the non-obese:obese observed ratio and the model was deemed able to predict the drug disposition changes in obese when the ratio between these two values was lower than twofold. For lorazepam the simulations in non-obese subjects were well predicted; however, the clearance was underpredicted in obese subjects. Therefore, we performed retrograde calculation to derive the change in enzymatic abundance for the uridine 5'-diphospho-glucuronosyltransferase enzyme (UGT), which resulted in an 18% increase in the obese group needed to match the observed clinical clearance value. To verify that the increase in enzyme abundance was valid across different substrates, we predicted the pharmacokinetics of other three UGT substrates, acetaminophen, dolutegravir, and raltegravir in both non-obese and obese individuals assuming that the impact of obesity on different UGT families is similar [23].

2.4 Analysis of the Main Pharmacokinetic Parameters Across Obesity

We used the ten developed drug models together with the previously published continuous functions describing the physiology of the obese population [13] to analyse the changes of the pharmacokinetic parameters across BMI, starting from 20 up to 60 kg/m^2, with BMI intervals of 2.5 kg/m^2. A total of 16 simulations per drug were run, each of them had 500 individuals (proportion of female: 0.5) split into ten different trials, and the dose used was the same as the one reported in Table 1. We calculated the mean peak concentration (C_{max}), time to C_{max} (t_{max}), apparent volume of distribution (V_d/F), apparent volume of distribution normalized by the total body weight (V_d/F/kg), area under the curve to the last time point (AUC_t), area under the curve to infinity (AUC_{inf}), apparent clearance (CL/F), and elimination half-life ($t_{1/2}$) for each simulation and normalized to the mean value of the lowest BMI group (20–22.5 kg/m^2). We investigated the association between BMI and pharmacokinetic parameters and examined when the latter changed more than the 1.25-fold interval (bioequivalence criterion and range within which changes in pharmacokinetic parameters are not considered clinically significant by the US Food and Drug Administration (FDA) and other regulatory bodies) [24, 25]. Furthermore, we investigated the correlation between hepatic blood flow and clearance of drugs hepatically metabolised and between the renal blood flow and clearance of renally eliminated drugs to evaluate how changes in these two physiological parameters impact clearance in obese subjects.

2.5 Sensitivity Analysis

We conducted a sensitivity analysis to further investigate the impact of the drug physicochemical properties on the volume of distribution. A drug file was created and it was populated with the mean physicochemical properties of the ten evaluated drugs. Simulations were run exploring six different types of drugs (neutral, weak acid pK_a = 9, moderate acid pK_a = 5, weak base pK_a = 5, intermediate base pK_a = 7.4, and moderate base pK_a = 9), BMI from 20 to 60 kg/m^2, and log$P$ from 5 to − 2, for a total of 816 simulations.

3 Results

3.1 Physiologically Based Pharmacokinetic Model Simulation Results in Obese Subjects

PBPK models for the ten selected drugs were developed and parametrized to predict both the observed concentration-time profiles and pharmacokinetic parameters in non-obese subjects. Then, the pharmacokinetics in obese subjects were simulated without changing the model parameters. Table 1 presents the clinical studies used for the model qualification in non-obese and obese subjects. Table 2 summarizes the observed and predicted pharmacokinetic parameters.

3.1.1 Midazolam

The benzodiazepine midazolam is mainly metabolized by cytochrome P450 (CYP) 3A (95.2%) and to a lesser extent by UGT1A1 (4.7%), while 0.1% is excreted in the urine [14]. Both intravenous and oral administration were simulated in non-obese and obese individuals. The clinically observed data for both groups and both administration routes were captured by the PBPK model; however, they did not fall exactly on the mean predicted profile because they represent single individual datapoints and therefore may not represent the clinical study mean (Fig. 1). The predicted:observed ratios for $t_{1/2}$ and AUC_{inf} were overpredicted in non-obese subjects (1.49 and 1.56) but were well captured in obese subjects (0.98 and 1.16). For oral administration, simulations for C_{max}, $t_{1/2}$, and AUC_{inf} were predicted for both non-obese and obese individuals within

Table 1 Summary of study design and anthropometric parameters mean (range) for the ten drugs used for the model qualification in non-obese and obese individuals

Drug	Drug class	Metabolic pathway	Dosing regimen	Non-obese individuals						Obese individuals					
				Reference	n	Age, y (range)	Proportion female	Weight, kg	BMI, kg/m² (range)	Reference	n	Age, y (range)	Proportion female	Weight, kg	BMI, kg/m² (range)
Midazolam	Benzodiazepine	CYP3A	5 mg, IVF, S.D.	[44]	40	33 (24–42)	0.43	64.68	21 (19–23)	[44]	20	36 (25–46)	0.35	116.5	38 (27–49)
Midazolam	Benzodiazepine	CYP3A	10 mg, PO, S.D.	[44, 45]	80	34 (25–42)	0.5	68.39	23 (20–27)	[44]	20	36 (25–46)	0.35	116.5	38 (27–49)
Triazolam	Benzodiazepine	CYP3A	0.5 mg, IVF, S.D.	[46]	15	24 (18–33)	0	78.9	25 (21–29)	[46]	12	27 (18–34)	0	111.9	36 (31–44)
Triazolam	Benzodiazepine	CYP3A	0.5 mg, PO, S.D.	[47]	9	NA (24–67)	0.33	64.2	22 (20–25)	[47]	9	NA (24–67)	0.44	119.7	41 (25–57)
Caffeine	Methylxanthine	CYP1A2	162 mg, PO, S.D	[48–50]	47	28 (22–35)	0.62	65.56	22 (19–25)	[48]	16	32 (24–40)	0.69	109	39 (28–50)
Chlorzoxazone	Miorilassant	CYP2E1	500 mg, PO, S.D.	[51, 52]	16	30 (26–43)	0.44	72.56	25 (22–29)	[51]	8	46 (37–55)	0.38	106.6	38 (31–44)
Acetaminophen	Analgesic	UGT/SULT	650 mg, IVF, S.D.	[53]	21	33 (23–62)	0.52	62.62	21 (19–25)	[53]	21	36 (23–59)	0.67	103.7	35 (25–60)
Acetaminophen	Analgesic	UGT/SULT	1000 mg PO, S.D.	[54, 55]	14	22 (19–25)	0	NA	22 (19–25)	[56]	10	44 (20–50)	0.9	137.7	49 (35–60)
Lorazepam	Benzodiazepine	UGT2B7/2B4/2B15	2 mg, IVB, S.D.	[57–60]	43	32 (22–43)	0.56	65.68	22 (19–26)	[57]	14	45 (23–66)	0.57	111.7	38 (26–60)
Propranolol	β-blocker	CYP2D6/2C19/1A2	10 mg, IVF, S.D.	[61, 62]	12	29 (25–34)	0.25	70.15	23 (21–24)	[61]	6	33 (27–39)	0.5	136.5	46 (42–50)
Propranolol	β-blocker	CYP2D6/2C19/1A2	40 mg PO, S.D.	[61, 63]	24	34 (31–37)	0.29	66.8	23 (21–24)	[61]	6	33 (27–39)	0.5	136.5	46 (42–50)
Amikacin	Aminoglycoside	GFR	500 mg, IVB, S.D. 1250 mg, IVB, S.D.	[64]	10	27 (22–32)	0.3	71	23 (19–27)	[65]	7	33 (21–48)	0.71	166.5	57 (43–63)
Tobramycin	Aminoglycoside	GFR*	331.5 mg, IVF, S.D. 346.5 mg, IVF, S.D.	[66]	8	23 (20–25)	0.5	66.3	22 (19–25)	[66]	20	43 (27–54)	0.55	137.8	42 (36–53)
Glimepiride	Antidiabetic	CYP2C9	8 mg, PO, S.D.	[67]	14	58 (42–69)	0.5	72.2	25 (19–31)	[67]	14	49 (37–63)	0.5	130	44 (39–57)

CYP cytochrome P450 enzyme, *GFR* glomerular filtration rate, *IVB* intravenous bolus administration, *IVF* intravenous infusion administration, *n* number of individuals, *NA* not available, *PO* oral administration, *S.D.* single dose, *UGT* Uridine 5′-diphospho-glucuronosyltransferase enzyme

*Observed tobramycin median (min–max) GFR based on urine collection were 124.7 (98–141) and 163.3 (85–230) mL/min in non-obese and obese, respectively; while the predicted GFR based on the equation reported by Berton et al. [8] and used in the simulation were 116.2 (88.4–162.8) and 147.9 (104.4–220.7) mL/min, respectively

the 1.5-fold margin and the ratios predicted:observed fold change between obese and non-obese were 0.94, 1.05, and 1.02, respectively (Table 2).

3.1.2 Triazolam

The benzodiazepine triazolam is metabolised exclusively via CYP3A4/5, and only a small part is excreted via glomerular filtration [15]. The 0.5 mg single intravenous infusion dose in both non-obese and obese subjects was well predicted by the model (Fig. 2a, b); the clinically observed data were in good agreement with the simulated concentration-time profiles, and the predicted:observed ratios for both $t_{1/2}$ and AUC_{inf} were within 1.25-fold. Oral triazolam predictions were all predicted within twofold (Fig. 2c, d); however by visual inspection it is clear that the model predictions are not in good agreement with the observed data, which may be explained by the fact that the observed data belong to a single non-obese individual (34-year-old male weighting 65 kg) and a single obese individual (34-year-old male weighting 159 kg). The predicted pharmacokinetic parameters in the virtual obese individuals were in agreement to observed data for $t_{1/2}$ (predicted:observed ratio: 1.14) but underpredicted for C_{max} and AUC_{inf} (0.6 and 0.57, respectively) (Table 2), probably due to some variability in the clinical study since the usual trend observed for all clinical data is a reduction in C_{max} and AUC_{inf}.

3.1.3 Caffeine

Caffeine is metabolised by CYP1A2 with only 1% eliminated unchanged in the urine [26]. The PBPK model simulations captured the observed clinical data in both non-obese and obese individuals well, with all concentration-time data falling within the 90% normal range (area within the 5th and 95th percentiles) of the simulated data (Fig. 3a, b). Predicted:observed ratios for C_{max}, $t_{1/2}$, and AUC_{inf} were all within 1.25-fold for both groups and the predicted pharmacokinetic changes were all in close agreement with the values obtained from the literature (Table 1).

3.1.4 Chlorzoxazone

Chlorzoxazone is metabolized by CYP2E1 [27]; its pharmacokinetics were studied after a single oral dose of 500 mg in both groups (Fig. 3c, d). The mean prediction was in agreement with the mean observed data; however, the observed pharmacokinetic variability was not completely captured by the model. The predicted:observed ratios in non-obese subjects were in good agreement for AUC_{inf} (0.92) but showed a slight underprediction for C_{max} and overprediction of $t_{1/2}$

(0.65 and 1.29, respectively), while for obese all three ratios were within 1.25-fold.

3.1.5 Acetaminophen

Acetaminophen is metabolised mainly by glucuronidation (~ 55%), sulphation (~ 30%), CYP2E1 (5–10%), and glomerular filtration (2–5%) [28]. The PBPK model was able to reproduce the pharmacokinetics of acetaminophen after intravenous and oral administration (Fig. 4). The observed fold change induced by obesity on the acetaminophen half-life was different between the intravenous and oral route of administration (0.89 and 1.7, respectively) (Table 2). On the other hand, the model predictions were consistent across the two routes, predicting a fold change of 1.51 and 1.69, respectively. Thus, the fold change for intravenous administration was overpredicted by the model (predicted:observed ratio = 1.77). All other pharmacokinetic parameter predictions in obese were in accordance with the observed data (all ratios were close to 1). For intravenous administration, the observed data in obese shown in Fig. 4b was based on a male subject with a BMI of 49 kg/m^2 and therefore may not be representative of the whole simulation and observed pharmacokinetic parameters (Table 2), which have a lower mean BMI (42 kg/m^2).

3.1.6 Lorazepam

Lorazepam is a benzodiazepine undergoing glucuronidation by UGT2B4, 2B7 and 2B15 [29]. Clinical data for both non-obese and obese subjects were available only for the intravenous route of administration. The PBPK model captured the disposition of lorazepam in both non-obese and obese subjects well (Fig. 5a, b). The ratio predicted:observed for $t_{1/2}$ and AUC_{inf} and the fold change in obese were well captured, with all ratios within 1.25-fold.

3.1.7 Propranolol

The beta-blocker propranolol is mainly metabolized by CYP2D6 (59%), CYP1A2 (21%), UGTs (17%) [20]. Clinically observed data were in good agreement with the simulations and all within the 90% prediction interval (Fig. 5c–f). All the pharmacokinetic parameters and the ratio of the predicted pharmacokinetic change in obese subjects were within 1.5-fold (Table 2).

3.1.8 Amikacin and Tobramycin

Amikacin and tobramycin are two aminoglycosides eliminated via glomerular filtration [30, 31]. The predicted and observed mean concentration-time profiles were in good agreement (Fig. 6a, b, c, d). Additionally, $t_{1/2}$ and AUC_{inf} for

**Table 2** Observed and predicted pharmacokinetic parameters in non-obese and obese individuals

		Non-obese individuals				Obese individuals				Ratio predicted/observed		Ratio obese/non obese		Ratio of (predicted ratio obese/non-obese)/(observed ratio obese/non-obese)
		Observed		Predicted		Observed		Predicted		Non-obese	Obese	Observed	Predicted	
		Mean	SD	Mean	SD	Mean	SD	Mean	SD					
Midazolam 5 mg IVF, S.D.														
BMI		19–23		19–23		27–49		27–49						
C_{max}	ng/mL													
$t_{1/2}$	h	2.5	1.2	3.8	1	8.4	3.8	8.2	2.1	1.49	0.98	3.31	2.18	0.66
AUC_{inf} CYP3A	ng*h/mL	155.4	42.1	242.5	49.4	176.6	63.6	205	43.5	1.56	1.16	1.14	0.85	0.75
Midazolam 10 mg PO, S.D.														
BMI		20–27		20–27		27–49		27–49						
C_{max}	ng/mL	71.2	32.9	50.2	15.4	64	35.7	42.7	14.4	0.71	0.67	0.9	0.85	0.94
$t_{1/2}$	h	3.8	4.8	4.8	1.4	5.9	3.8	7.9	1.6	1.26	1.33	1.58	1.66	1.05
AUC_{inf} CYP3A	ng*h/mL	166	103.2	155	53.3	141.2	63.6	134.9	45.7	0.93	0.95	0.85	0.87	1.02
Triazolam 0.5 mg IVF, S.D.														
BMI		21–29		21–29		31–44		31–44						
C_{max}	ng/mL													
$t_{1/2}$	h	3.9	1.1	3.8	1	4.7	1.5	5.1	1.3	0.98	1.09	1.2	1.32	1.1
AUC_{inf} CYP3A	ng*h/mL	43.9	8.5	53.3	17.5	45	12.3	46.1	14.6	1.21	1.02	1.02	0.86	0.84
Triazolam 0.5 mg PO, S.D.														
BMI		20–25		20–25		25–57		25–57						
C_{max}	ng/mL	3.7	1.8	3.3	0.7	4.6	1.2	2.5	0.6	0.89	0.53	1.24	0.75	0.6
$t_{1/2}$	h	2.6	0.7	3.9	1.6	4.1	1.7	7.2	3.5	1.53	1.74	1.61	1.83	1.14
AUC_{inf} CYP3A	ng*h/mL	16.4	4.8	21.2	12	27.7	9.6	20.2	14.6	1.29	0.73	1.69	0.96	0.57
Caffeine 162 mg PO, S.D.														
BMI		19–25		19–25		28–50		28–50						
C_{max}	ng/mL	4613	1264	4630	1039	2702		3488	986	1	1.29	0.59	0.75	1.27
$t_{1/2}$	h	5.6	2.8	5.7	1	7	4.3	7.6	1.3	1.01	1.09	1.26	1.35	1.07
AUC_{inf} CYP1A2	ng*h/mL	26512	50039	30578	5651	20000	8296	24233	4688	1.15	1.21	0.75	0.79	1.05
Chlorzoxazone 500 mg PO, S.D.														
BMI		22–29		22–29		31–44		31–44						
C_{max}	ng/mL	12373	5297	8470	1443	5200	2200	5100	930	0.68	0.98	0.42	0.6	1.43
$t_{1/2}$	h	1	0.5	1.3	0.1	1.4	0.9	1.4	0.1	1.29	0.99	1.4	1.07	0.76
AUC_{inf} CYPC2E1	ng*h/mL	36750	20851	33974	7506	15700	11300	19443	3968	0.92	1.24	0.43	0.57	1.33
Acetaminophen 650 mg IVF, S.D.														
BMI		19–25		19–25		25–60		25–60						
C_{max}	ng/mL													
$t_{1/2}$	h	2.7	0.3	2.9	0.6	2.4	0.4	4.2	1	1.06	1.77	0.89	1.51	1.7
AUC_{inf} UGT/SULT	ng*h/mL	40969	11351	53377	11665	30609	8332	41441	11778	1.30	1.35	0.75	0.8	1.07
Acetaminophen 1,000 mg PO, S.D.														
BMI		19–25		19–25		35–60		35–60						
C_{max}	ng/mL	15774	6541	16172	3631	12333	4800	11432	2853	1.03	0.93	0.78	0.71	0.91
$t_{1/2}$	h	2.7	0.5	2.7	0.7	4.6	0.8	4.5	0.9	1	0.99	1.7	1.69	0.99
AUC_{inf} UGT/SULT	ng*h/mL	42853	9287	56503	20967	35333	10133	43327	14111	1.32	1.23	0.82	0.77	0.94

Table 2 (continued)

			Non-obese individuals				Obese individuals				Ratio predicted/observed		Ratio obese/non obese		Ratio of (predicted obese/non-obese)/(observed obese/non-obese)
			Observed		Predicted		Observed		Predicted		Non-obese	Obese	Observed	Predicted	
			Mean	SD	Mean	SD	Mean	SD	Mean	SD					
Lorazepam	BMI		19–26		19–26		26–60		26–60						
2 mg	C_{max}	ng/mL													
IVB, S.D.	$t_{1/2}$	h	14.8	4.3	15.4	11.8	16.5	6.7	19.5	9.8	1.04	1.18	1.11	1.26	1.14
UGT2B7/2B4/2B15	AUC_{inf}	ng*h/mL	503.4	184.8	559.7	402.3	326.8	122.3	312.2	180.8	1.11	0.96	0.65	0.56	0.86
Propranolol	BMI		21–24		21–24		42–50		42–50						
10 mg	C_{max}	ng/mL													
IVF, S.D.	$t_{1/2}$	h	3.3	0.6	3.8	0.6	5	0.7	6.2	0.7	1.17	1.25	1.52	1.62	1.07
CYP2D6/2C19/1A2	AUC_{inf}	ng*h/mL	209.7	31.4	288.9	47.5	213.68	13.42	237.17	39.06	1.38	1.11	1.02	0.82	0.8
Propranolol	BMI		21–24		21–24		42–50		42–50						
40 mg	C_{max}	ng/mL	36.1	8.9	40.7	9.7	31.0	4.9	29.5	7.3	1.13	0.95	0.86	0.72	0.84
PO, S.D.	$t_{1/2}$	h	3.2	0.5	3.9	0.5	4.9	1.2	6.1	0.7	1.19	1.24	1.51	1.57	1.04
CYP2D6/2C19/1A2	AUC_{inf}	ng*h/mL	225	56	277.9	70.7	260	61	233.6	58.9	1.23	0.9	1.15	0.84	0.73
Amikacin	BMI		19–27		19–27		43–60		43–60						
500 mg	C_{max}	ng/mL													
IVB, S.D.	$t_{1/2}$	h	1.9	0.4	2	0.2	2.2	0.6	2.5	0.3	1.06	1.13	1.17	1.25	1.07
GFR	AUC_{inf}	ng*h/mL	82194	18905	89080	12948	55509	15542	63152	8230	1.08	1.14	0.68	0.71	1.04
Tobramycin	BMI		19–25		19–25		36–53		36–53						
331.5 mg	C_{max}	ng/mL													
IVF, S.D.	$t_{1/2}$	h	2.3	0.6	2.5	0.2	3.3	1.0	3.2	0.4	1.09	0.96	1.44	1.27	0.88
GFR	AUC_{inf}	ng*h/mL	70000	12000	71388	8433	51021	14824	53850	7705	1.02	1.06	0.73	0.75	1.03
Glimepiride	BMI		19–31		19–31		39–57		39–57						
8 mg	C_{max}	ng/mL	547	218	485	101	410	124	296	53	0.89	0.72	0.75	0.61	0.81
PO, S.D.	$t_{1/2}$	h	3.4	1.1	3.2	2.1	4.4	1.9	4.3	2.1	0.93	0.98	1.28	1.35	1.05
CYP2C9	AUC_{inf}	ng*h/mL	3205	1033	3284	1775	2818	1112	2403	952	1.02	0.85	0.88	0.73	0.83

AUC_{inf} area under the curve to infinity, *CYP* cytochrome P450 enzyme, C_{max} peak concentration, *GFR* glomerular filtration rate, *IVB* intravenous bolus administration, *IVF* intravenous infusion administration, *PO* oral administration, *S.D.* single dose, *SD* standard deviation, $t_{1/2}$ elimination half-life, *UGT* Uridine 5′-diphospho-glucuronosyltransferase enzyme

Fig. 1 Simulations for midazolam intravenous infusion in non-obese (**a**) and obese (**b**) individuals and for oral midazolam in non-obese (**c**) and obese (**d**) individuals. The red markers depict the observed clinical data, while the solid lines, bold solid line, and shaded area represent the mean of each virtual trial, the mean of all trials, and the 90% normal range, respectively, of all virtual individuals
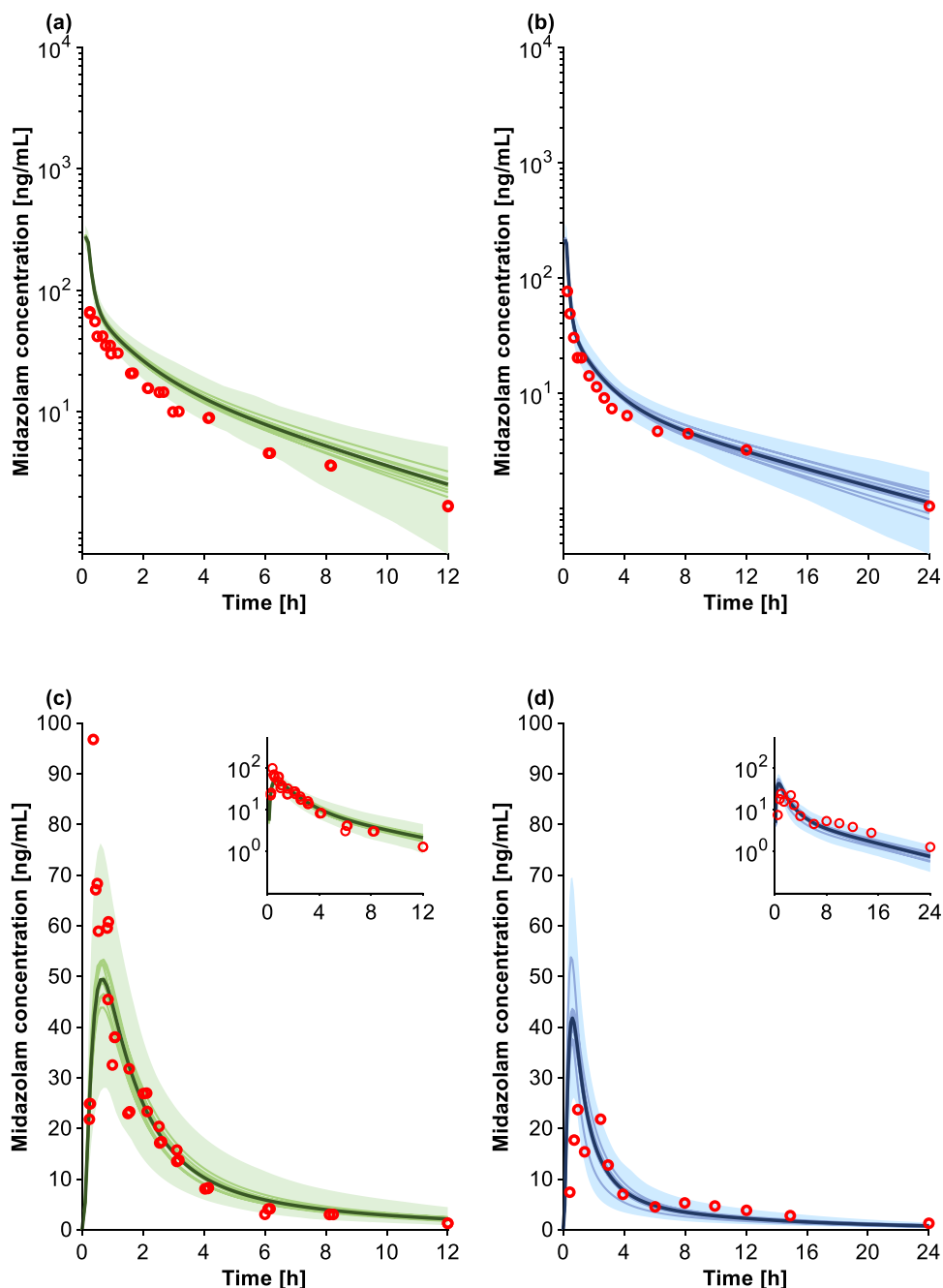
both drugs and both groups were predicted within the 1.25-fold margin.

3.1.9 Glimepiride

The antidiabetic drug glimepiride is metabolized entirely by CYP2C9 [32]. The clinically observed data for both non-obese and obese subjects were within the 90% normal range of the predicted data (Fig. 6e, f). The predicted:observed ratios for C_{max}, $t_{1/2}$, and AUC_{inf} were all within the 1.25-fold margin apart from the C_{max} in obese, which was slightly underpredicted but nonetheless within the 1.5-fold margin. The fold

change in the pharmacokinetic parameters in obese were in agreement with the observed ratios and all within the 1.25-fold margin.

3.1.10 Summary

Overall, the predicted pharmacokinetic parameters were within 1.25-fold (71.5%), 1.5-fold (21.5%) and twofold (7%) of clinical data, while none were outside the twofold error margin. These results clearly demonstrate the ability of the PBPK framework [9], informed with our developed obese

Fig. 2 Simulations for triazolam intravenous infusion in non-obese (**a**) and obese (**b**) individuals and for oral triazolam in non-obese (**c**) and obese (**d**) individuals. The red markers depict the observed clinical data, while the solid lines, bold solid line, and shaded area represent the mean of each virtual trial, the mean of all trials, and the 90% normal range, respectively, of all virtual individuals
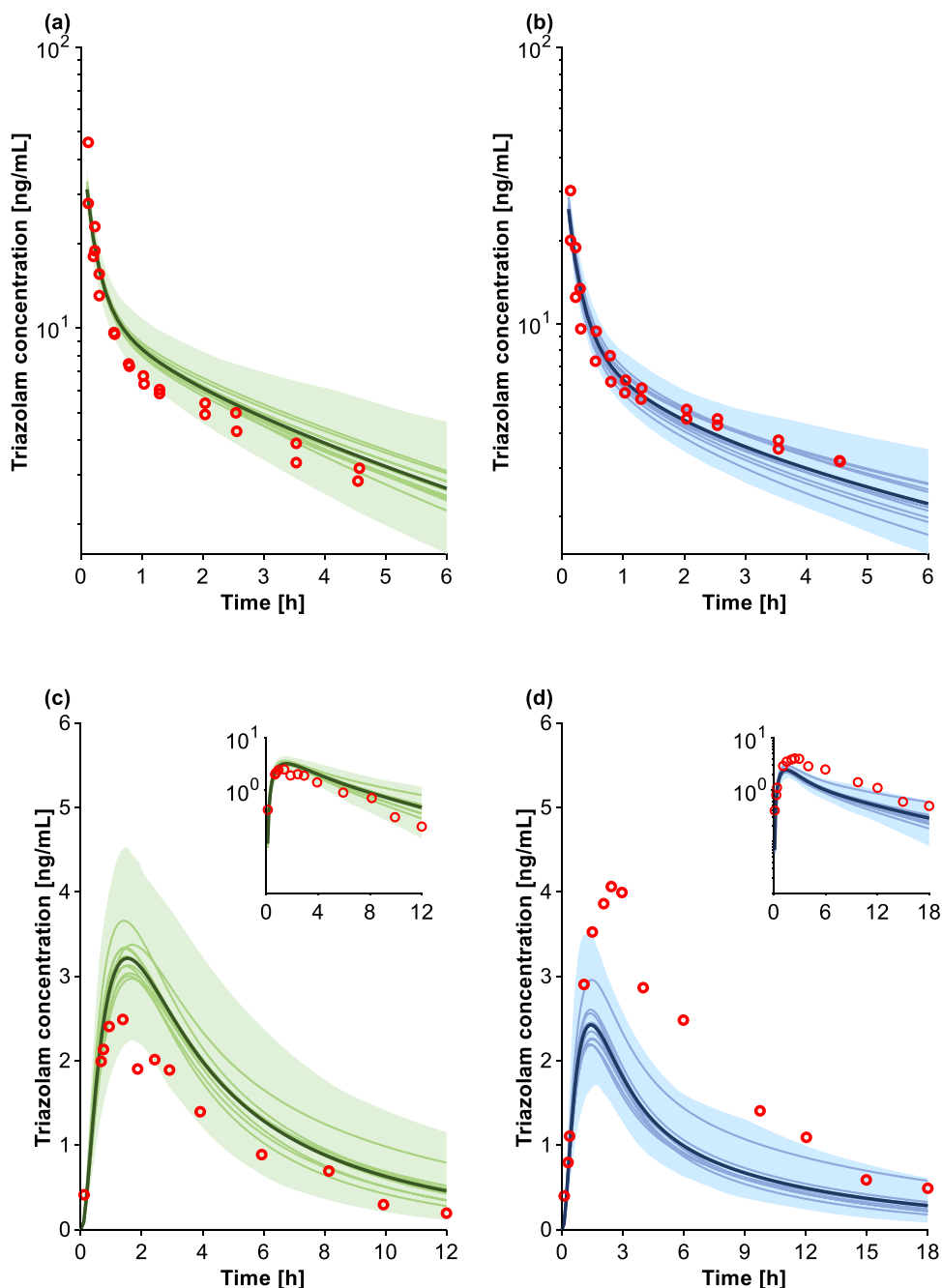
population [13], to reliably predict drug disposition in this special population.

3.2 Pharmacokinetic Parameters Driving Drug Exposure Changes in Obese Subjects

3.2.1 Pharmacokinetic Parameter Changes from BMI 20 to 60 kg/m²

After verifying the capability of the model to predict the pharmacokinetics in obese subjects, we used the model to investigate the continuous effect of obesity on the pharmacokinetic parameters of the ten studied drugs. Figure 7 illustrates the results of the analysis, each colour and marker represents a drug. Compounds are organized based on the $\log P$ value with midazolam (yellow ochre colour) having the highest and amikacin (green) the lowest value. C_{max} was found to decrease similarly across all drugs by 1.5% per BMI unit regardless of the drug type and $\log P$ (Fig. 7a). T_{max} on the other hand was not hugely impacted by obesity and the fold change in t_{max} was still within the bioavailability ranges (Fig. 7b). The volume of distribution (Fig. 7g) markedly

Fig. 3 Simulations for oral caffeine in non-obese (**a**) and obese (**b**) individuals and for oral chlorzoxazone in non-obese (**c**) and obese (**d**) individuals. The red markers depict the observed clinical data (mean ± SD), while the solid lines, bold solid line, and shaded area represent the mean of each virtual trial, the mean of all trials, and the 90% normal range, respectively, of all virtual individuals
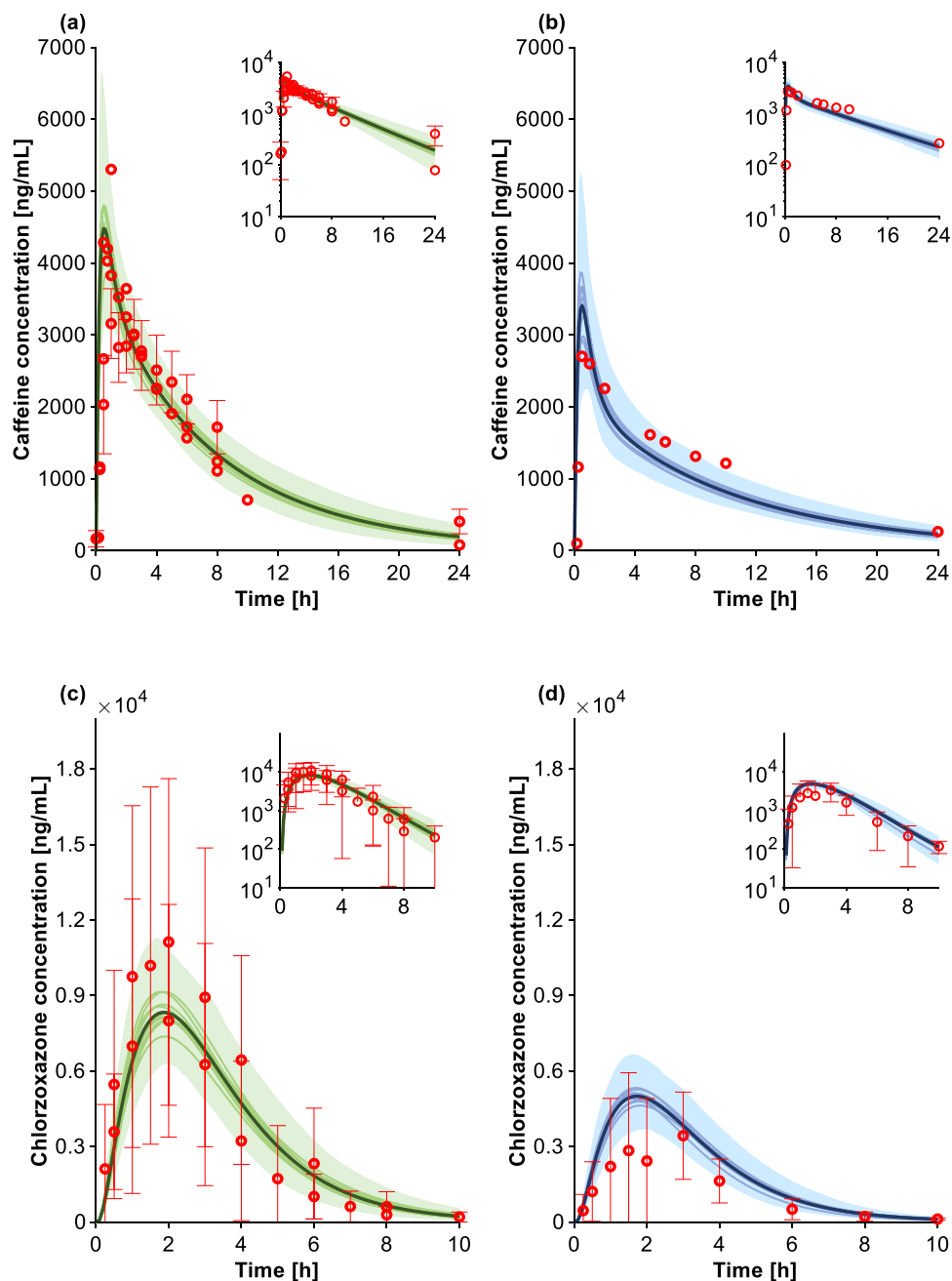
increased for all medications, going outside the bioavailability range at a BMI of 25 kg/m^2 and reaching on average threefold higher values in individuals with a BMI of 60 kg/m^2. However, the increase in volume of distribution was very variable, being the lowest for drugs such as amikacin and tobramycin with a 3% increase per BMI unit and the highest for midazolam with a 9% increase per BMI unit. The volume of distribution normalized by the total body weight (TBW) (Fig. 7h) showed better the differences in distribution across drugs. Midazolam and lorazepam had the steepest increase,

meaning that the volume of distribution increases more than TBW, while for acetaminophen and caffeine it was constant, indicating a parallel increase between the two. Conversely, it decreased for tobramycin and amikacin, suggesting that the volume of distribution does not increase as much as TBW. Clearance was shown to increase by 1.6% for each BMI unit, reaching 64% increase in individuals with a BMI of 60 kg/m^2 (Fig. 7f). Lorazepam was the compound with the highest clearance in obese subjects with an increase of 2.8% per BMI unit, while triazolam had the least steep increase, 0.6%

Fig. 4 Simulations for acetaminophen intravenous infusion in non-obese (**a**) and obese (**b**) individuals and for oral acetaminophen in non-obese (**c**) and obese (**d**) individuals. The red markers depict the observed clinical data (mean ± SD), while the solid lines, bold solid line, and shaded area represent the mean of each virtual trial, the mean of all trials, and the 90% normal range, respectively, of all virtual individuals
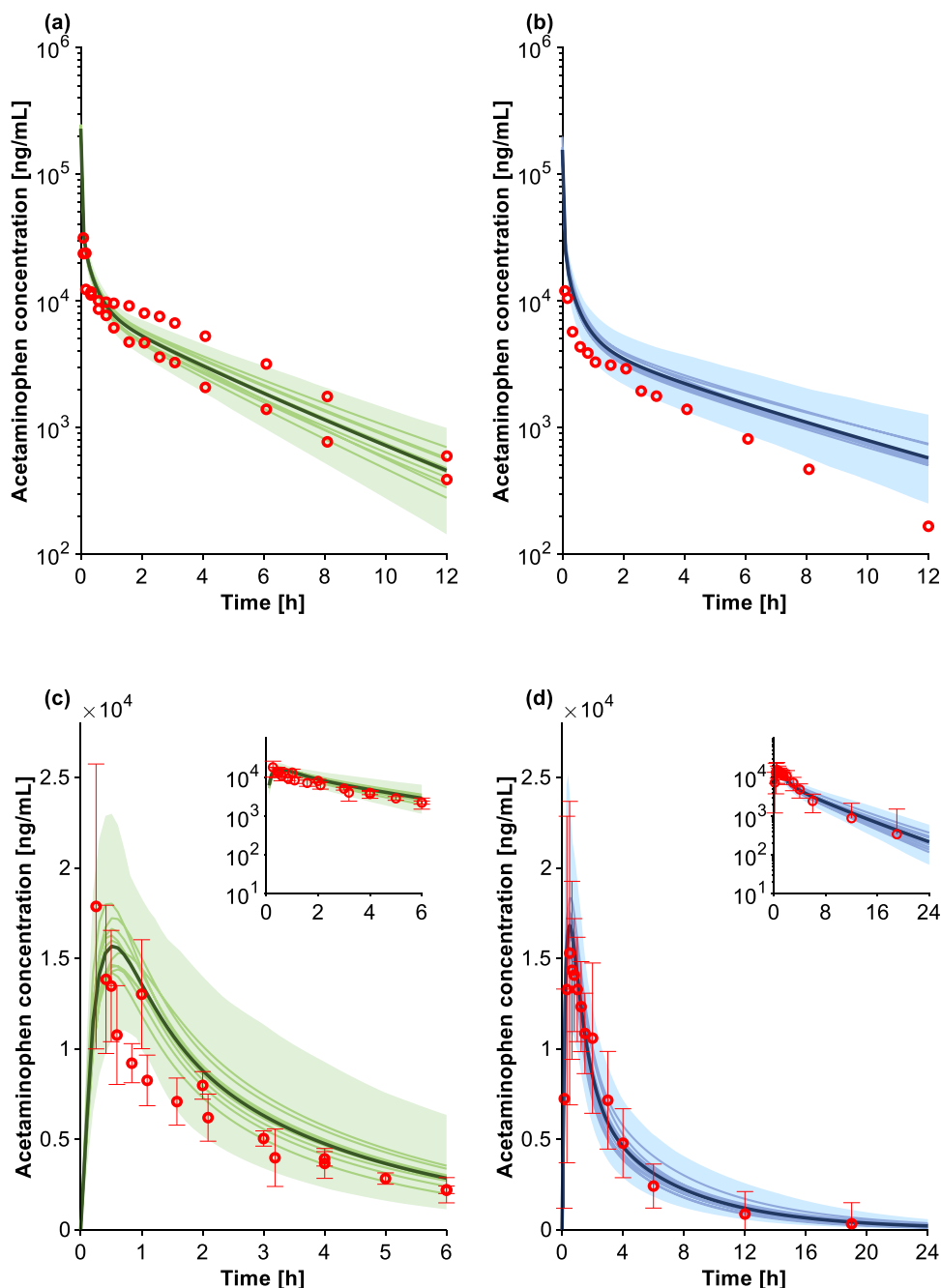
per BMI value. The trendline for clearance showed that the bioequivalence range was surpassed at a BMI of 35 kg/m². Since AUC_{inf} is correlated to clearance, it was shown to decrease across BMI values at a similar percentage to that of clearance (Fig. 7e). Larger differences among drugs were observed when considering AUC_{inf} (Fig. 7e) compared to AUC_t (Fig. 7d). Half-life is a secondary parameter derived from the ratio between the volume of distribution and clearance. Even if both primary parameters were found to increase

with increasing BMI, the rate of increase for the volume of distribution was higher compared to clearance, leading to a rise in $t_{1/2}$ of about 2.4% per BMI unit (Fig. 7c). For drugs with a higher volume of distribution, $t_{1/2}$ was even higher (i.e., midazolam and triazolam). However, in the case of lorazepam there was a better balance between volume of distribution and clearance, thereby mitigating the increase in $t_{1/2}$.

To further investigate the impact of the liver and renal blood flows on the clearance of the studied drugs, two
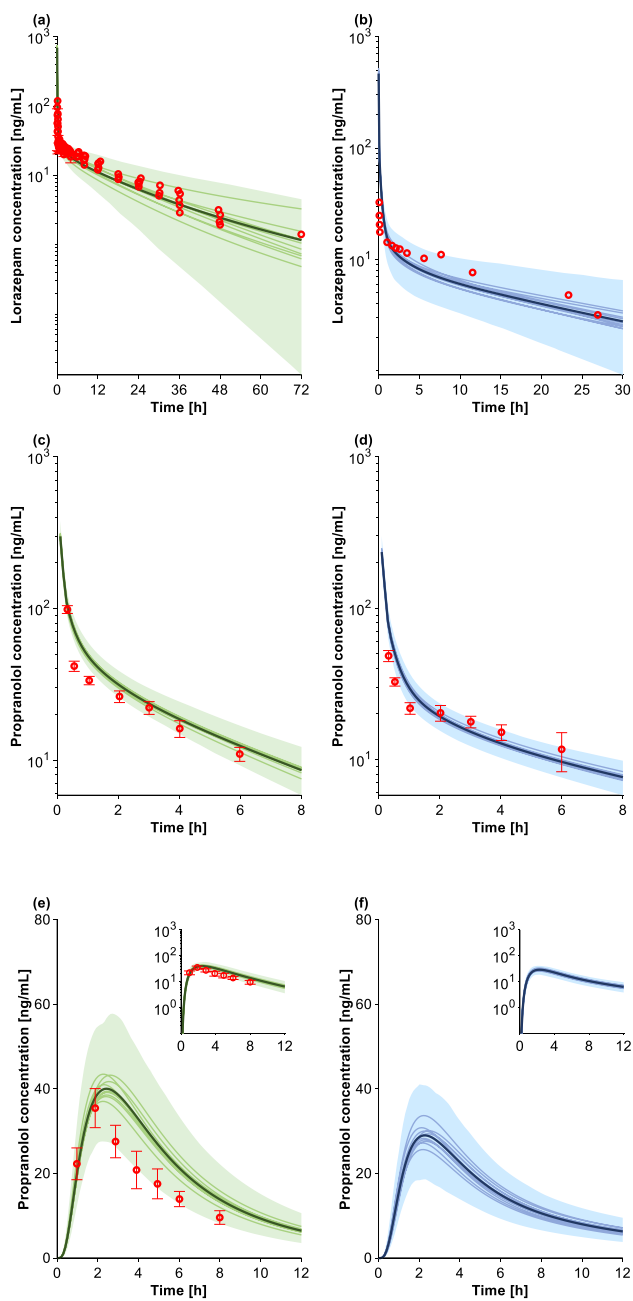
Fig. 5 Simulations for lorazepam intravenous bolus in non-obese (**a**) and obese (**b**) individuals, for propranolol intravenous infusion in non-obese (**c**) and obese (**d**) individuals, and for oral propranolol in non-obese (**e**) and obese (**f**) individuals. The red markers depict the observed clinical data (mean ± SD), while the solid lines, bold solid line, and shaded area represent the mean of each virtual trial, the mean of all trials, and the 90% normal range, respectively, of all virtual individuals

Fig. 6 Simulations for amikacin intravenous bolus in non-obese (**a**) and obese (**b**) individuals, for tobramycin intravenous infusion in non-obese (**c**) and obese (**d**) individuals, and for oral glimepiride in non-obese (**e**) and obese (**f**) individuals. The red markers depict the observed clinical data (mean ± SD), while the solid lines, bold solid line, and shaded area represent the mean of each virtual trial, the mean of all trials, and the 90% normal range, respectively, of all virtual individuals

correlation plots were generated (Fig. 8). The trend-lines for both liver blood flow and clearance and renal blood flow and clearance were very close to the identity line, suggesting that the increase in clearance is mostly explained by the increase in liver and renal blood flow.

For the drugs metabolized by the liver, different trends were observed for lorazepam and triazolam, both trends relating to the altered enzyme abundance (i.e., higher for UGT resulting in elevated clearance for lorazepam

and lower for CYP3A resulting in reduced clearance for triazolam).

3.2.2 Sensitivity Analysis to Investigate the Effect of Drug Characteristics on the Volume of Distribution

The plots correlating volume of distribution and BMI (Fig. 7g, h) indicate that lipophilicity is not the only physicochemical parameter influencing the distribution of a drug. This is supported by the fact that the volume of distribution of the lipophilic drug glimepiride does not increase as much as other drugs with similar $\log P$ values (i.e., midazolam). Therefore, we investigated the interplay between $\log P$ and pK_a on the volume of distribution. As depicted in the three-dimensional (3D) plots (Fig. 9), the increase in volume of distribution with increasing BMI is driven by $\log P$ for a neutral compound. For instance, for a $\log P$ of -2, V_d/F changes by 2.5-fold when considering a BMI of 60 kg/m^2 compared to 20 kg/m^2; however, the change goes up to 3.7-fold for a drug with a $\log P$ of 5. The same behaviour is observed for drugs with a weak acid ($pK_a = 9$) or basic ($pK_a = 5$) group (Fig. 9b, d) since the unionized form is the dominant one. However, for a moderate acid ($pK_a = 5$) or base ($pK_a = 9$), the behaviour changes; V_d/F does still increase with higher BMI values, however $\log P$ is not the driving parameter given that the drug is present in the ionized form. Lastly, for a basic compound whose pK_a is equal to the physiological pH (in which case the drug is half ionized and unionized), the drug behaves similarly to a neutral drug but $\log P$ has a lower impact. In summary, pK_a is the driving factor for the increase in volume of distribution for ionized compounds whereas $\log P$ plays a more important role for neutral and unionized compounds.

4 Discussion

Despite the high prevalence of obese individuals worldwide, there is a paucity of data on how to adjust the dosage of medications, the main reason being the under-representation of this special population from clinical trials [6]. In this study, the pharmacokinetics of ten drugs eliminated through different pathways were successfully predicted a priori in obese subjects using our PBPK framework informed with our obese population repository [13], thereby demonstrating the predictive power of this approach to predict drug disposition in special populations.

The general trend for the ten evaluated drugs was a decrease in C_{max} and AUC, an increase in volume of distribution, clearance, and half-life, and an unchanged t_{max}.

However, the effect of obesity on the pharmacokinetics was different across drugs. The volume of distribution was generally greater for drugs with a high $\log P$ such as midazolam, lorazepam, and triazolam. Drugs with a $\log P$ around 0 such as acetaminophen and caffeine showed an intermediate behaviour, while renally eliminated hydrophilic drugs such as tobramycin and amikacin distributed the least in the adipose tissue [33]. However, not all drugs followed this trend. Although propranolol, glimepiride, and chlorzoxazone have a $\log P$ of 3.48, 3.12, and 1.94, respectively, their volume of distribution did not increase as much as other compounds with a similar $\log P$ such as midazolam or triazolam. We could demonstrate in the sensitivity analysis that this difference relates to pK_a. Glimepiride, a mono acid with a pK_a of 4.32, behaves similarly to Fig. 9c, while the basic compounds propranolol and chlorzoxazone with pK_a values of 9.5 and 9.39, respectively, behave similarly to Fig. 9e. We demonstrated that for compounds mostly ionized at physiological pH, $\log P$ is not representative of the drug behaviour in obese subjects. $\log P$ expresses the lipophilicity of a compound in the unionized state. However, in a physiological system with a pH of about 7.4, a compound can ionize, therefore $\log D_{7.4}$ ($\log D$ at pH 7.4) becomes a better indicator of the drug lipophilicity. Thus, $\log D_{7.4}$ can characterize better changes in the volume of distribution in obese subjects, indeed the $\log D_{7.4}$ for propranolol, glimepiride and chlorzoxazone are 1.20, 1.33 and 1.19, respectively [34, 35]. Indeed, $\log D$ (but not $\log P$) better predicts the permeability of compounds across membranes [36].

Another critical parameter that we investigated was clearance, which increased for all drugs albeit to various extents. Drugs that followed similar patterns were those undergoing metabolism by enzymes unaltered by obesity. Conversely, drugs metabolized by enzymes whose abundance is changed in obese subjects (i.e., UGT and CYP3A) had a different pattern [13, 37, 38]. Of interest, midazolam clearance did not change as much as that of triazolam. This observation may be explained by the higher hepatic extraction rate of midazolam compared to triazolam so that midazolam is more sensitive to changes in hepatic blood flow rather than enzyme abundance. We could also demonstrate that the main physiological drivers for the elevated metabolic and renal clearance are the increased hepatic and renal blood flows in obese individuals. These two physiological parameters were also identified in our previous work as being the key drivers for the decreased clearance in elderly [39]. Since metabolism is increased in obese subjects, the AUCs of drugs tend to decrease, and due to the higher elimination half-life, AUC$_{inf}$ was shown to better describe differences in drug exposure. Finally, we
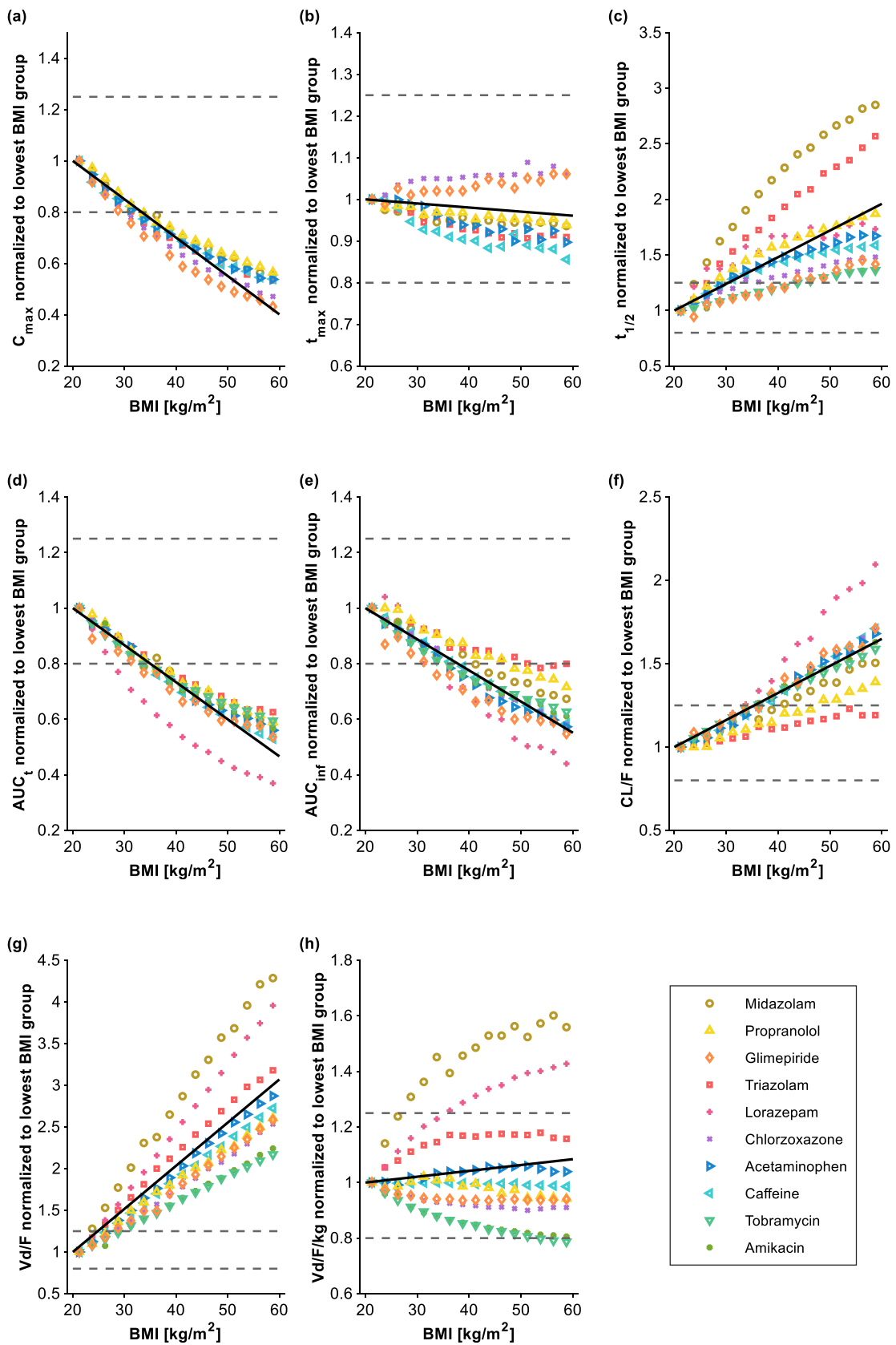
◀**Fig. 7** Pharmacokinetic parameters fold change across body mass index (BMI) range 20–60 kg/m² for the ten studied drugs. The pharmacokinetic values are normalized to smallest BMI value. The regression line describing the parameter trend is represented in black, while the interindividual variability range defined as the 1.25-fold interval (bioequivalence criterion) is delimited by the two grey dotted lines. C_{max} peak concentration, t_{max} time to C_{max}, V_d/F apparent volume of distribution, AUC_{inf} area under the curve to infinity, CL/F clearance, $t_{1/2}$ elimination half-life

showed that C_{max} decreased across all drugs; however, the difference among drugs was minimal.

The current study presents some limitations. The clinical data and the virtual obese population used in this study represent people affected by obesity but otherwise healthy. Therefore, our results might not be transposable to obese individuals with an additional disease condition (i.e., renal or hepatic impairment [40, 41]) that might alter the physiology and consequently drug pharmacokinetics. Additionally, the virtual obese population has a validity age range between 20 to 50 years, so we could not use it to simulate and investigate pharmacokinetics in elderly obese subjects. The PBPK model in some cases (i.e., chlorzoxazone) was not able to fully capture the observed variability, possibly due to formulations or absorption differences between studies, which the model was not able to capture due to the basic absorption module. Furthermore, in our sensitivity analysis, we looked at two main physicochemical properties – $\log P$ and pK_a; however, other important drug parameters might influence the volume of distribution, such as the polar surface area, molecular weight, hydrogen bond donor, hydrogen bond acceptor, and the fraction of unbound in plasma.

5 Conclusions

The current study further confirms the ability of PBPK modelling to predict drug pharmacokinetics in special populations such as the obese [39, 42, 43]. It also provides additional proof that our previously published repository containing continuous functions describing anatomical, physiological, and biological parameters generates virtual obese populations that can be reliably used to reproduce the drug disposition in obese. Drug exposure changes in obese subjects are due to increases in clearance and volume of distribution. The increase in clearance was driven by an increase in hepatic and renal blood flows, and differences across drugs could be explained by the altered enzymatic abundance. The volume of distribution was higher in obese subjects for all drugs; however, different trends could not be explained by the $\log P$, instead $\log D_{7.4}$ was a better descriptor of lipophilicity in a physiological system since it considers the ionization of the compound. The study also highlights that the physiological changes and physicochemical parameters of the drug both play a role in the drug disposition in obese subjects, therefore making it difficult to have a fixed rule for scaling doses from non-obese to obese. PBPK modelling takes into consideration both the physiology and physicochemical properties, and can be used to simulate virtual clinical trials for those drugs for which clinical data are still not available in the obese, thereby filling the pharmacokinetic knowledge gap still present in the literature.

Fig. 8 Correlation plots between clearance and hepatic blood flow (**a**), and clearance and renal blood flow (**b**). The clearance and blood flow values are normalized to the smallest body mass index (BMI) value. The regression line describing the parameter trend is represented in black while the red dashed line is the line of unity. CL/F clearance, Qh hepatic blood flow, Qr renal blood flow
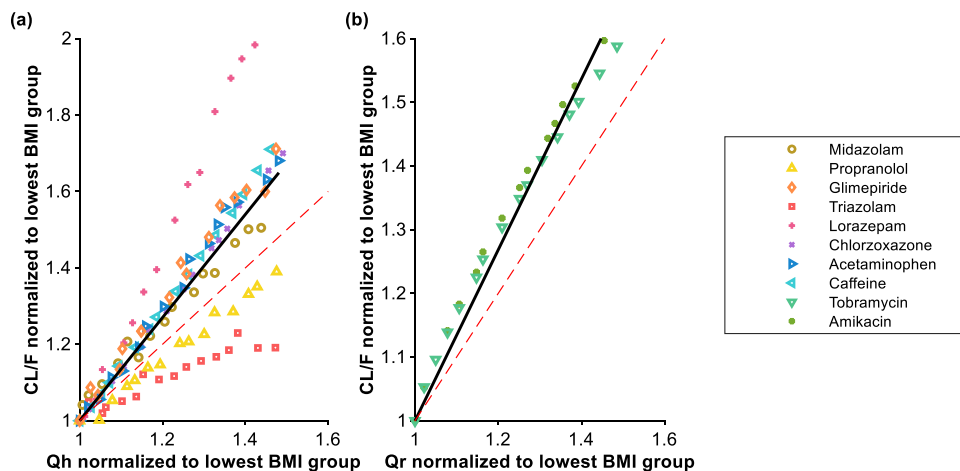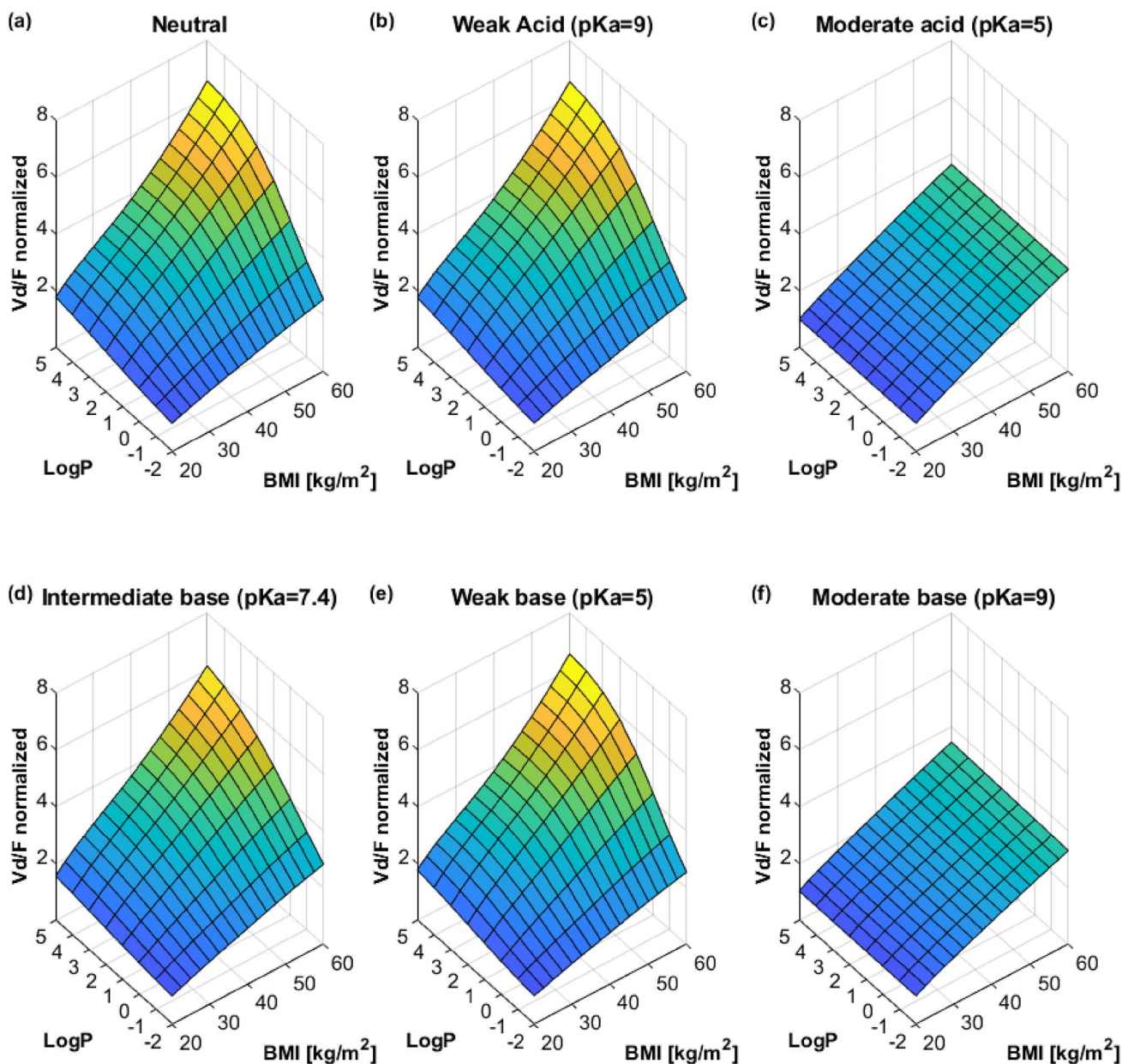
Fig. 9 Three-dimensional plot illustration the impact of log$P$ and body mass index (BMI) on volume of distribution for neutral (**a**), weak acid (**b**), moderate acid (**c**), intermediate base (**d**), weak base (**e**), and moderate base (**f**). V_d/F apparent volume of distribution, log$P$ octanol-water partition coefficient

the study and supervised the data analysis. MBa provided clinical input. CM designed the study, supervised the data analysis, and obtained the funding. All authors contributed to the critical review and approval of the manuscript.

Consent to participate Not applicable

Consent for publication Not applicable

References

1. World Health Organization. https://www.who.int/news-room/fact-sheets/detail/obesity-and-overweight. Accessed 4 Nov 2021.
2. Collaborators GBDO, Afshin A, Forouzanfar MH, Reitsma MB, Sur P, Estep K, et al. Health effects of overweight and obesity in 195 countries over 25 years. N Engl J Med. 2017;377(1):13–27.
3. Ng M, Fleming T, Robinson M, Thomson B, Graetz N, Margono C, et al. Global, regional, and national prevalence of overweight and obesity in children and adults during 1980–2013: a systematic analysis for the Global Burden of Disease Study 2013. Lancet. 2014;384(9945):766–81.
4. Hruby A, Hu FB. The epidemiology of obesity: a big picture. Pharmacoeconomics. 2015;33(7):673–89.
5. Fruh SM. Obesity: risk factors, complications, and strategies for sustainable long-term weight management. J Am Assoc Nurse Pract. 2017;29(S1):S3–14.
6. Jain R, Chung SM, Jain L, Khurana M, Lau SW, Lee JE, et al. Implications of obesity for drug therapy: limitations and challenges. Clin Pharmacol Ther. 2011;90(1):77–89.
7. Smit C, De Hoogd S, Bruggemann RJM, Knibbe CAJ. Obesity and drug pharmacology: a review of the influence of obesity on pharmacokinetic and pharmacodynamic parameters. Expert Opin Drug Metab Toxicol. 2018;14(3):275–85.
8. Berton M, Bettonte S, Stader F, Battegay M, Marzolini C. Repository describing the anatomical, physiological, and biological changes in an obese population to inform physiologically based pharmacokinetic models. Clin Pharmacokinet. 2022;61(9):1251–70.
9. Stader F, Penny MA, Siccardi M, Marzolini C. A comprehensive framework for physiologically based pharmacokinetic modelling in Matlab. CPT Pharmacomet Syst Pharmacol. 2019 Feb 18;8(7):444–59.
10. Rodgers T, Leahy D, Rowland M. Physiologically based pharmacokinetic modeling 1: predicting the tissue distribution of moderate-to-strong bases. J Pharm Sci. 2005;94(6):1259–76.
11. Rodgers T, Rowland M. Physiologically based pharmacokinetic modelling 2: predicting the tissue distribution of acids, very weak bases, neutrals and zwitterions. J Pharm Sci. 2006;95(6):1238–57.
12. Stader F, Siccardi M, Battegay M, Kinvig H, Penny MA, Marzolini C. Repository describing an aging population to inform physiologically based pharmacokinetic models considering anatomical, physiological, and biological age-dependent changes. Clin Pharmacokinet. 2019;58(4):483–501.
13. Berton M, Bettonte S, Stader F, Battegay M, Marzolini C. Repository describing the anatomical, physiological, and biological changes in an obese population to inform physiologically based pharmacokinetic models. Clin Pharmacokinet. 2022; (**in press**).
14. Rowland Yeo K, Walsky RL, Jamei M, Rostami-Hodjegan A, Tucker GT. Prediction of time-dependent CYP3A4 drug-drug interactions by physiologically based pharmacokinetic modelling: impact of inactivation parameters and enzyme turnover. Eur J Pharm Sci. 2011;43(3):160–73.
15. Chetty M, Rose RH, Abduljalil K, Patel N, Lu G, Cain T, et al. Applications of linking PBPK and PD models to predict the impact of genotypic variability, formulation differences, differences in target binding capacity and target site drug concentrations on drug responses and variability. Front Pharmacol. 2014;5:258.
16. Darakjian LI, Kaddoumi A. Physiologically based pharmacokinetic/pharmacodynamic model for caffeine disposition in pregnancy. Mol Pharm. 2019;16(3):1340–9.
17. Li J, Guo HF, Liu C, Zhong Z, Liu L, Liu XD. Prediction of drug disposition in diabetic patients by means of a physiologically based pharmacokinetic model. Clin Pharmacokinet. 2015;54(2):179–93.
18. Jiang XL, Zhao P, Barrett JS, Lesko LJ, Schmidt S. Application of physiologically based pharmacokinetic modeling to predict acetaminophen metabolism and pharmacokinetics in children. CPT Pharmacomet Syst Pharmacol. 2013;16(2): e80.
19. Maharaj AR, Barrett JS, Edginton AN. A workflow example of PBPK modeling to support pediatric research and development: case study with lorazepam. AAPS J. 2013;15(2):455–64.
20. Rose RH, Turner DB, Neuhoff S, Jamei M. Incorporation of the time-varying postprandial increase in splanchnic blood flow into a PBPK model to predict the effect of food on the pharmacokinetics of orally administered high-extraction drugs. AAPS J. 2017;19(4):1205–17.
21. Ferreira A, Martins H, Oliveira JC, Lapa R, Vale N. PBPK Modeling and simulation of antibiotics amikacin, gentamicin, tobramycin, and vancomycin used in hospital practice. Life (Basel). 2021;11(11):1130.
22. Shebley M, Sandhu P, Emami Riedmaier A, Jamei M, Narayanan R, Patel A, et al. Physiologically based pharmacokinetic model qualification and reporting procedures for regulatory submissions: a consortium perspective. Clin Pharmacol Ther. 2018;104(1):88–110.
23. Berton M, Bettonte S, Decosterd L, Battegay M, Cavassini M, Stader F, et al. Pharmacokinetics of Dolutegravir And Bictegravir in Obese People Living With HIV [Poster-G01]. Conference on retroviruses and opportunistic infections. February 12–16, 2022.
24. U.S. Food and Drug Administration. Department of Health and Human Services. Bioequivalence Studies With Pharmacokinetic Endpoints for Drugs Submitted Under an ANDA Guidance for Industry. (2021)
25. European Medicines Agency. Committee for medicinal products for human use. Guideline on the investigation of bioequivalence. (2010)
26. Blanchard J, Sawers SJ. Comparative pharmacokinetics of caffeine in young and elderly men. J Pharmacokinet Biopharm. 1983;11(2):109–26.
27. Peter R, Boecker R, Beaune PH, Iwasaki M, Guengerich FP, Yang CS. Hydroxylation of chlorzoxazone as a specific probe

for human liver cytochrome P-450IIE1. Chem Res Toxicol. 1990;3(6):566–73.

28. van Rongen A, Välitalo PAJ, Peeters MYM, Boerma D, Huisman FW, van Ramshorst B, et al. Morbidly obese patients exhibit increased CYP2E1-mediated oxidation of acetaminophen. Clin Pharmacokinet. 2016;55(7):833–47.

29. Elliott HW. Metabolism of lorazepam. Br J Anaesth. 1976;48(10):1017–23.

30. U.S. Food and Drug Administration. Amikacin NDA. 1997. https://www.accessdata.fda.gov/drugsatfda_docs/nda/97/64146AP.PDF. Accessed 11 Apr 2022.

31. U.S. Food and Drug Administration. Tobramycin NDA. 2003. https://www.accessdata.fda.gov/drugsatfda_docs/nda/2004/050789s000_Tobramycin_PharmR.pdf. Accessed 11 Apr 2022.

32. Prescribing information. Amaryl (glimepiride). Bridgewater, NJ: Aventis Pharmaceutical Products. 2000; https://products.sanofi.us/amaryl/amaryl.pdf. Accessed 11 Apr 2022.

33. Abernethy DR, Greenblatt DJ. Drug disposition in obese humans. An update Clin Pharmacokinet. 1986;11(3):199–213.

34. Dave RA, Morris ME. A quantitative threshold for high/low extent of urinary excretion of compounds in humans. Biopharm Drug Dispos. 2016;37(5):287–309.

35. Benet LZ, Broccatelli F, Oprea TI. BDDCS applied to over 900 drugs. AAPS J. 2011;13(4):519–47.

36. Kokate A, Li X, Jasti B. Effect of drug lipophilicity and ionization on permeability across the buccal mucosa: a technical note. AAPS PharmSciTech. 2008;9(2):501–4.

37. Ulvestad M, Skottheim IB, Jakobsen GS, Bremer S, Molden E, Asberg A, et al. Impact of OATP1B1, MDR1, and CYP3A4 expression in liver and intestine on interpatient pharmacokinetic variability of atorvastatin in obese subjects. Clin Pharmacol Ther. 2013;93(3):275–82.

38. Krogstad V, Peric A, Robertsen I, Kringen MK, Vistnes M, Hjelmesaeth J, et al. Correlation of body weight and composition with hepatic activities of cytochrome P450 enzymes. J Pharm Sci. 2021;110(1):432–7.

39. Stader F, Kinvig H, Penny MA, Battegay M, Siccardi M, Marzolini C. Physiologically based pharmacokinetic modelling to identify pharmacokinetic parameters driving drug exposure changes in the elderly. Clin Pharmacokinet. 2020;59(3):383–401.

40. Eknoyan G. Obesity and chronic kidney disease. Nefrologia. 2011;31(4):397–403.

41. Carr RM, Oranu A, Khungar V. Nonalcoholic fatty liver disease: pathophysiology and management. Gastroenterol Clin North Am. 2016;45(4):639–52.

42. Abduljalil K, Pansari A, Jamei M. Prediction of maternal pharmacokinetics using physiologically based pharmacokinetic models: assessing the impact of the longitudinal changes in the activity of CYP1A2, CYP2D6 and CYP3A4 enzymes during pregnancy. J Pharmacokinet Pharmacodyn. 2020;47(4):361–83.

43. Heimbach T, Chen Y, Chen J, Dixit V, Parrott N, Peters SA, et al. Physiologically-based pharmacokinetic modeling in renal and hepatic impairment populations: a pharmaceutical industry perspective. Clin Pharmacol Ther. 2021;110(2):297–310.

44. Greenblatt DJ, Abernethy DR, Locniskar A, Harmatz JS, Limjuco RA, Shader RI. Effect of age, gender, and obesity on midazolam kinetics. Anesthesiology. 1984;61(1):27–35.

45. Lam YW, Alfaro CL, Ereshefsky L, Miller M. Pharmacokinetic and pharmacodynamic interactions of oral midazolam with ketoconazole, fluoxetine, fluvoxamine, and nefazodone. J Clin Pharmacol. 2003;43(11):1274–82.

46. Derry CL, Kroboth PD, Pittenger AL, Kroboth FJ, Corey SE, Smith RB. Pharmacokinetics and pharmacodynamics of triazolam after two intermittent doses in obese and normal-weight men. J Clin Psychopharmacol. 1995;15(3):197–205.

47. Abernethy DR, Greenblatt DJ, Divoll M, Smith RB, Shader RI. The influence of obesity on the pharmacokinetics of oral alprazolam and triazolam. Clin Pharmacokinet. 1984;9(2):177–83.

48. Abernethy DR, Todd EL, Schwartz JB. Caffeine disposition in obesity. Br J Clin Pharmacol. 1985;20(1):61–6.

49. Kaplan GB, Greenblatt DJ, Ehrenberg BL, Goddard JE, Cotreau MM, Harmatz JS, et al. Dose-dependent pharmacokinetics and psychomotor effects of caffeine in humans. J Clin Pharmacol. 1997;37(8):693–703.

50. Cysneiros RM, Farkas D, Harmatz JS, von Moltke LL, Greenblatt DJ. Pharmacokinetic and pharmacodynamic interactions between zolpidem and caffeine. Clin Pharmacol Ther. 2007;82(1):54–62.

51. Wang Z, Hall SD, Maya JF, Li L, Asghar A, Gorski JC. Diabetes mellitus increases the in vivo activity of cytochrome P450 2E1 in humans. Br J Clin Pharmacol. 2003;55(1):77–85.

52. Hohmann N, Blank A, Burhenne J, Suzuki Y, Mikus G, Haefeli WE. Simultaneous phenotyping of CYP2E1 and CYP3A using oral chlorzoxazone and midazolam microdoses. Br J Clin Pharmacol. 2019;85(10):2310–20.

53. Abernethy DR, Divoll M, Greenblatt DJ, Ameer B. Obesity, sex, and acetaminophen disposition. Clin Pharmacol Ther. 1982;31(6):783–90.

54. Rawlins MD, Henderson DB, Hijab AR. Pharmacokinetics of paracetamol (acetaminophen) after intravenous and oral administration. Eur J Clin Pharmacol. 1977;11(4):283–6.

55. Kamali F, Edwards C, Rawlins MD. The effect of pirenzepine on gastric emptying and salivary flow rate: constraints on the use of saliva paracetamol concentrations for the determination of paracetamol pharmacokinetics. Br J Clin Pharmacol. 1992;33(3):309–12.

56. Chen KF, Chan LN, Senn TD, Oelschlager BK, Flum DR, Shen DD, et al. The impact of Proximal Roux-en-Y gastric bypass surgery on acetaminophen absorption and metabolism. Pharmacotherapy. 2020;40(3):191–203.

57. Abernethy DR, Greenblatt DJ, Divoll M, Shader RI. Enhanced glucuronide conjugation of drugs in obesity: studies of lorazepam, oxazepam, and acetaminophen. J Lab Clin Med. 1983;101(6):873–80.

58. Greenblatt DJ, Shader RI, Franke K, MacLaughlin DS, Harmatz JS, Allen MD, et al. Pharmacokinetics and bioavailability of intravenous, intramuscular, and oral lorazepam in humans. J Pharm Sci. 1979;68(1):57–63.

59. Greenblatt DJ, Divoll M, Harmatz JS, Shader RI. Pharmacokinetic comparison of sublingual lorazepam with intravenous, intramuscular, and oral lorazepam. J Pharm Sci. 1982;71(2):248–52.

60. Wermeling DP, Miller JL, Archer SM, Manaligod JM, Rudy AC. Bioavailability and pharmacokinetics of lorazepam after intranasal, intravenous, and intramuscular administration. J Clin Pharmacol. 2001;41(11):1225–31.

61. Bowman SL, Hudson SA, Simpson G, Munro JF, Clements JA. A comparison of the pharmacokinetics of propranolol in obese and normal volunteers. Br J Clin Pharmacol. 1986;21(5):529–32.

62. Regardh CG, Johnsson G, Jordo L, Lungborg P, Persson BA, Ronn O. Plasma concentrations and beta-blocking effects in normal volunteers after intravenous doses of metoprolol and propranolol. J Cardiovasc Pharmacol. 1980;2(6):715–23.

63. Mould GP, Clough J, Morris BA, Stout G, Marks V. A propranolol radioimmunoassay and its use in the study of its pharmacokinetics following low doses. Biopharm Drug Dispos. 1981;2(1):49–57.

64. Walker JM, Wise R, Mitchard M. The pharmacokinetics of amikacin and gentamicin in volunteers: a comparison of individual differences. J Antimicrob Chemother. 1979;5(1):95–9.

65. Bauer LA, Blouin RA, Griffen WO Jr, Record KE, Bell RM. Amikacin pharmacokinetics in morbidly obese patients. Am J Hosp Pharm. 1980;37(4):519–22.

66. Smit C, Wasmann RE, Wiezer MJ, van Dongen HPA, Mouton JW, Bruggemann RJM, et al. Tobramycin clearance is best described by renal function estimates in obese and non-obese individuals: results of a prospective rich sampling pharmacokinetic study. Pharm Res. 2019;36(8):112.

67. Shukla UA, Chi EM, Lehr KH. Glimepiride pharmacokinetics in obese versus non-obese diabetic patients. Ann Pharmacother. 2004;38(1):30–5.

Authors and Affiliations

Mattia Berton[1,2] ⬤ **· Sara Bettonte[1,2] · Felix Stader[3] · Manuel Battegay[1,2] · Catia Marzolini[1,2,4]**

✉ Mattia Berton
  mattia.berton@unibas.ch

[1] Division of Infectious Diseases and Hospital Epidemiology, Departments of Medicine and Clinical Research, University Hospital Basel, Basel, Switzerland

[2] University of Basel, Basel, Switzerland

[3] Certara UK Limited, Sheffield, UK

[4] University of Liverpool, Liverpool, UK